Journal of Fluorescence (2019) 29:121–135
https://doi.org/10.1007/s10895-018-2316-2

ORIGINAL ARTICLE

Fluorescent 7-Substituted Coumarin Dyes: Solvatochromism and NLO Studies

Archana A. Bhagwat[1] · Nagaiyan Sekar[1]

Received: 28 August 2018 / Accepted: 14 October 2018 / Published online: 29 October 2018

Abstract

The effect of three substituents N,N-diethylamine, carbazole and diphenylamine at the 7 position of coumarin on linear and nonlinear optical properties are studied using absorption and emission solvatochromism, and DFT. By varying the substituent 53 nm red shift is achieved in emission. The polarity plots with regression close to unity revealed good charge transfer in the system. Solvent polarizability and dipolarity are mainly responsible for solvatochromic shift as proved by multilinear regression analysis. General Mulliken Hush analysis shows diphenylamine substituent leads to more charge separation in compound 6c. The hyperpolarizabilities are evaluated by quantum mechanical calculations. Structure of the compounds are optimized at B3LYP/6-31G(d) level and NLO computations are done using range separated hybrid functionals with large basis sets. Second order hyperpolarizability (γ) found 589.27 × 10^{-36}, 841.29 × 10^{-36} and 1043.00 × 10^{-36} e.s.u for the compounds 6a, 6b and 6c respectively.

Keywords Coumarin · Solvatochromism · DFT · Hyperpolarizability

Introduction

Solvent polarity dependent change in intensity and position in spectra is termed as solvatochromism. It is divided into subtype, positive and negative solvatochromism [1]. Bathochromic shift in emission is known as positive solvatochromism and a hypsochromic shift in emission is known as negative solvatochromism. Solvatochromism is governed by the structural changes of the compounds and solvent environment. The effect of solvent medium on photophysical properties of the coumarin dyes are well explored [2, 3]. 7-Aminocoumarins are applied in electronics and biological field [4–7]. Solvatochromic Push-Pull (D-π-A) chromophores show intramolecular charge transfer (ICT) [8]. The absorption-emission properties of 7-substituted coumarin chromophore can be tuned by changing the substituents at seventh position. 7-Substituted coumarin shows a significant change in emission intensity, Stokes shift and quantum yield in varying polarity solvents [9–11].

The photochemistry of the solvatochromic compounds is studied by different solvatochromic models. Lippert, Dimroth, Catalan and Kamlet Taft model are well known and widely used [12–15]. Lippert model useful for estimation of excited state dipole moment. Knowledge of excited state dipole moment is important to design nonlinear optical materials [16]. Coumarin dyes found applicable in optoelectronics [17, 18]. The highly fluorescent, solvatochromic, large Stokes shifted compounds are attracted our attention. Among dye class, coumarins are known as highly fluorescent chromophore so we have chosen chromophore core for our study. To get solvatochromism and high Stokes shift we have altered substituent at the C_7 position.

In this study, we have shown the effect of three different 7-substituted coumarins on photophysical properties. Solvatochromic study of synthesized dyes is done using Lippert-mataga solvent polarity scale, multilinear regression analysis which involves Kamlet-Taft and Catalan method. Excited state dipole moment and hyperpolarizabilies are derived using solvatochromic and computational approach.

Electronic supplementary material The online version of this article (https://doi.org/10.1007/s10895-018-2316-2) contains supplementary material, which is available to authorized users.

✉ Nagaiyan Sekar
nethi.sekar@gmail.com

[1] Department of Dyestuff Technology, Institute of Chemical Technology, Matunga, Mumbai 400 019, India

Experimental

Materials and Methods

All the starting materials were obtained from S.D. Fine Chemical and Sigma-Aldrich and used without further purification. Synthetic grade solvents used. Anton Paar monowave 400 microwave used for the coupling reaction. Precoated 0.25 mmE.Merck silica gel 60 F254 thin layer chromatography plates were used for monitoring the reaction. Instrument from Sunder industrial product was used in measuring the melting points, and are uncorrected. NMR spectra were obtained from Agilent 500 MHz instrument using $CDCl_3$ and DMSO-d_6. The chemical shifts are reported in parts per million (ppm) relative to internal standard tetramethyl silane (TMS) (0 ppm) and coupling constants in Hz. Perkin-Elmer Lambda 25 UV-Visible spectrophotometer was used for recording visible absorption spectra at the fixed concentration on. Emissions were recorded on Cary Eclipse spectrophotometer at 5 slit width. Quantum yield was calculated by using fluorescein as standard.

Synthesis

Aldehyde 5a and 5c are synthesized according to a literature procedure [19, 20]. Aldehyde 5b is synthesized as shown in synthetic scheme 1.

Compound 2 is obtained by the known method [21]. Methylation is carried out using DMS as follows,

Synthesis of compound **3**: 4-iodo-2-methoxybenzaldehyde

Under nitrogen, 2-hydroxy-4-iodobenzaldehyde (0.093 mmol) and sodium carbonate (2.8 mmol) were taken in RB flask with acetone to it DMS (1.8 mmol) was added. The reaction mixture was refluxed for 12 h. After completion of reaction, sodium carbonate was filtered out. The remaining solution was concentrated on rota evaporator. Yield: 40%. Mp. 84-86 °C.

^{1}H NMR (500 MHz, $CdCl_3$) δ 10.41 (s, 1H), 7.51 (d, J = 8.1 Hz, 1H), 7.42 (ddd, J = 8.2, 1.3, 0.7 Hz, 1H), 7.37 (d, J = 1.3 Hz, 1H), 3.93 (s, 3H).

Synthesis of compound 4: 4-(9H-carbazol-9-yl)-2-methoxybenzaldehyde

To a magnetically stirred solution of carbazole (0.89 mmol) in 1,2-dichloro benzene (0.2 ml) 4-iodo-2-methoxybenzaldehyde 3 (0.89 mmol), K_2CO_3 (2.67 mmol), Cu (0.44 mmol) and 18-crown-6 (1.78 mmol) were added in 10 ml microwave tube. The mixture was degassed with nitrogen for about 30 min and then heated at 200 °C for 20 min in the microwave. The temperature of the reaction mixture was brought down, filtered and evaporated giving a brown oil which was treated with hexane and left overnight with constant magnetic stirring to elute impurities. The hexane layer was discarded and the residue was purified by column using hexane: ethyl acetate (10:1) as an eluent. Yield 46%. Mp. 138-140 °C.

^{1}H NMR (500 MHz, $CdCl_3$) δ 10.51 (s, 1H), 8.14 (d, J = 7.7 Hz, 2H), 8.07 (d, J = 8.2 Hz, 1H), 7.52 (d, J = 8.2 Hz, 2H), 7.45–7.42 (m, 2H), 7.34–7.30 (m, 2H), 7.29 (dd, J = 8.2, 1.2 Hz, 1H), 7.23 (d, J = 1.7 Hz, 1H), 3.96 (s, 3H).

^{13}C NMR (126 MHz, $CdCl_3$) δ 188.66, 162.90, 144.68, 140.02, 130.21, 126.27, 123.90, 123.39, 120.72, 120.49, 118.73, 109.89, 109.67, 56.02.

Synthesis of compound 5b: 4-(9H-carbazol-9-yl)-2-hydroxybenzaldehyde

4-(9H-Carbazol-9-yl)-2-methoxybenzaldehyde **4** (0.16 mmol) was dissolved in 0.5 g of pyridine. HCl and heated to 185 °C for 1.5 h. On cooling to room temperature water was added in the reaction mass and solid precipitated out was filtered, and dried. The compound obtained was purified by column chromatography using hexane: ethyl acetate (10:1) as the eluent to get the pure product.

Yield 50%. Mp. 140-144 °C.

^{1}H NMR (500 MHz, DMSO-d_6) δ 11.10 (s, 1H), 10.31 (s, 1H), 8.22 (d, J = 7.8 Hz, 2H), 7.89 (d, J = 8.8 Hz, 1H), 7.53 (d, J = 8.3 Hz, 2H), 7.45–7.41 (m, 2H), 7.29 (t, J = 7.4 Hz, 2H), 7.22 (dd, J = 4.4, 2.4 Hz, 2H).

^{1}H NMR (500 MHz, DMSO-d_6 and D_2O) δ 10.29 (s, 1H), 8.21 (d, J = 7.7 Hz, 2H), 7.89 (d, J = 8.8 Hz, 1H), 7.52 (d, J = 8.2 Hz, 2H), 7.45–7.41 (m, 2H), 7.28 (t, J = 7.4 Hz, 2H), 7.22 (dq, J = 3.6, 1.8 Hz, 2H).

^{13}C NMR (125 MHz, DMSO-d_6) δ 190.37, 162.37, 144.01, 139.64, 131.04, 126.94, 123.68, 121.65, 121.21, 121.09, 117.49, 114.39, 110.53.

Synthesis of 6a, 6b and 6c (Fig. 1)

Aldehydes 5a-5c (1 mmol) and 7-(diethylamino)-2-oxobenzo[d]thiazole-2-carbonitrile (1 mmol) were stirred in absolute ethanol (5 mL) for a period of 4–5 h in presence of piperidine (0.01 ml). Reaction was monitored by TLC. On completion of reaction, solution was mixed with ice water (20 mL) containing 0.025 mL of conc. HCl. The precipitate was filtered and washed with water, dried under vacuum to give compounds 6a-6c.

6a: 3-(Benzo[d]thiazol-2-yl)-7-(diethylamino)-2H-chromen-2-one: Red solid, mp obtained 198-202 °C. Reported 208-210 °C.

Elemental Analysis Found: C, 68.59; H, 5.18; N, 7.98%; molecular formula $C_{20}H_{18}N_2O_2S$ requires C, 68.55; H, 5.18; N, 7.99%.

Scheme 1 Synthetic scheme for compound 6a, 6b and 6c

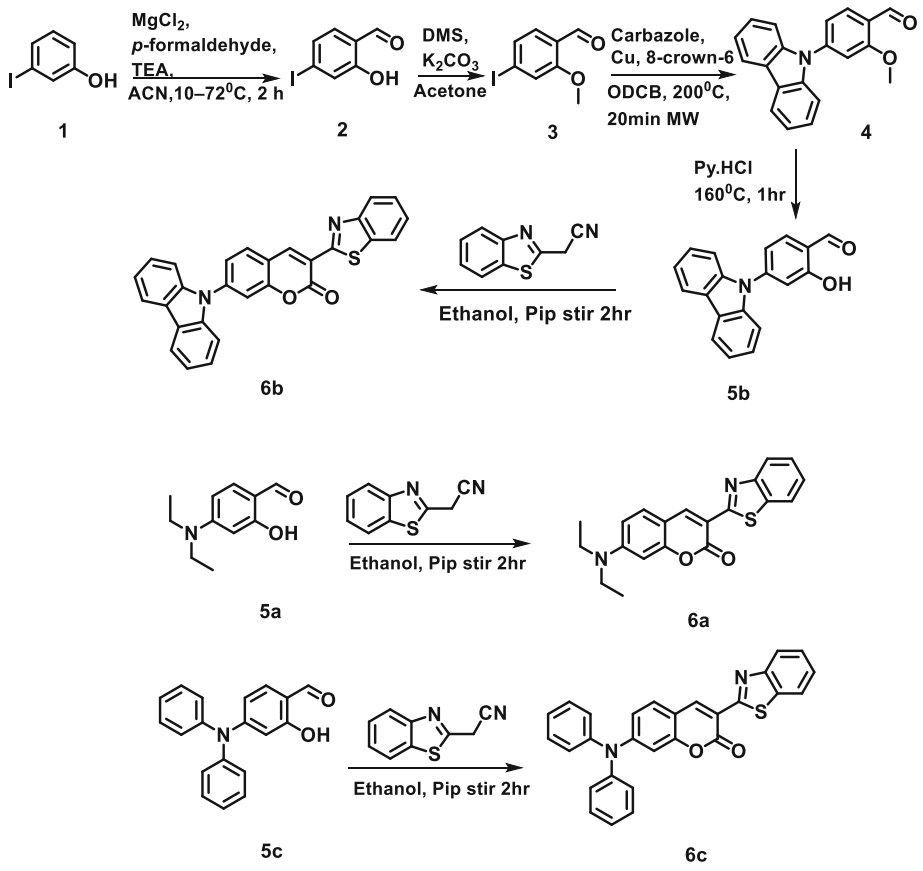

6b: 3-(Benzo[d]thiazol-2-yl)-7-(9H-carbazol-9-yl)-2H-chromen-2-one: reddish orange solid, mp 194-196 °C.

^{1}H NMR (500 MHz, DMSO-d_6) δ 9.37 (d, J = 1.8 Hz, 1H), 8.34 (d, J = 8.3 Hz, 1H), 8.27 (d, J = 7.8 Hz, 1H), 8.20 (d, J = 8.0 Hz, 1H), 8.12 (d, J = 8.1 Hz, 1H), 7.89 (s, 1H), 7.79 (d, J = 8.3 Hz, 1H), 7.60 (dd, J = 9.8, 4.7 Hz, 1H), 7.50 (qd, J = 8.1, 1.0 Hz, 1H), 7.35 (t, J = 7.5 Hz, 1H).

^{13}C NMR (125 MHz, DMSO-d_6) δ 160.18, 159.85, 154.90, 152.39, 141.96, 141.76, 139.84, 136.37, 132.31, 127.30, 127.13, 126.06, 123.78, 123.50, 123.02, 122.75, 121.51, 121.13, 119.56, 118.11, 114.06, 110.47.

Elemental Analysis Found: C, 75.69; H, 3.63; N, 6.31%; molecular formula $C_{28}H_{16}N_2O_2S$ requires C, 75.66; H, 3.63; N, 6.30%.

6c: 3-(Benzo[d]thiazol-2-yl)-7-(diphenylamino)-2H-chromen-2-one: yellowish orange solid, mp 244-246 °C.

^{1}H NMR (500 MHz, $CdCl_3$) δ 8.95 (s, 1H), 8.05 (d, J = 8.2 Hz, 1H), 7.97 (d, J = 8.1 Hz, 1H), 7.51 (dd, J = 8.2, 7.1 Hz, 1H), 7.47 (d, J = 8.7 Hz, 1H), 7.44–7.35 (m, 5H), 7.23 (d, J = 7.3 Hz, 6H), 6.93 (dd, J = 8.7, 0.9 Hz, 1H), 6.86 (s, 1H).

^{13}C NMR (125 MHz, $CdCl_3$) δ 160.97, 160.44, 155.81, 152.93, 152.47, 145.44, 141.41, 136.48, 129.92, 126.63, 126.24, 125.87, 124.82, 122.40, 121.64, 121.21, 116.59, 115.39, 112.15, 105.18.

Elemental Analysis Found: C, 75.36; H, 4.06; N, 6.28%; molecular formula $C_{28}H_{16}N_2O_2S$ requires C, 75.32; H, 4.06; N, 6.27%.

Fig. 1 Structure of the compounds synthesized

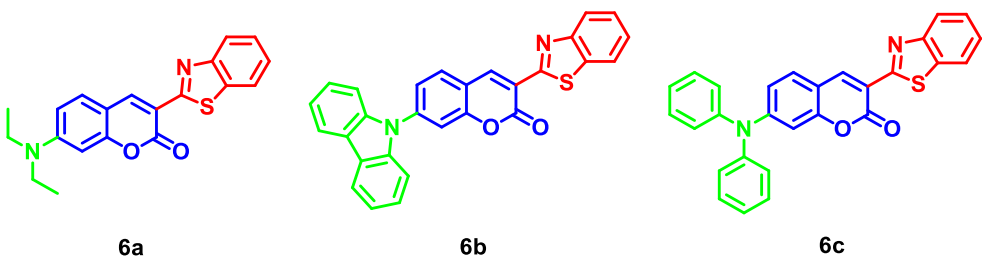

Result and Discussion

Photophysical Properties

Synthesized compounds solvatochromic response was studied in nine different polarity solvents. Compounds 6a, 6b and 6c absorb in range of 406 nm - 460 nm and emission in the range of 480 nm - 598 nm (Fig. 2). In chloroform compounds 6a, 6b and 6c absorbed at 444 nm, 408 nm and 453 nm respectively (Table 1). Among three compounds compound 6c having diphenyl amine substituent shows the highest molar absorptivity. All the compounds show positive solvatochromism in emission. Compounds 6a, 6b and 6c show emission maxima in 492 nm, 511 and 544 nm chloroform. Compound 6a shows twisted intramolecular charge transfer transition (TICT) in polar protic solvents [22, 23]. Emission intensity decreases as solvent polarity increases which indicates that intramolecular charge transfer (ICT) state stabilized by polar solvents. Compound 6b shows larger FWHM 129 nm and Stokes shift 153 nm in acetonitrile. Large stokes shift for 6b and 6c indicates the ground state and excited state geometry could be different in these compounds. Quantum yield found more in nonpolar solvents. Compound 6a shows the highest quantum yield. Radiative and non-radiative decay in different solvent studied using Strickler Berg Eq. [25].

$$K_r = 2.88 \times 10^{-9} n^2 < \bar{\upsilon}_f^{-3} >_{Av^{-1}} \frac{g1}{g2} \int \varepsilon d \ln \bar{\upsilon} \tag{1}$$

where n and $< \bar{\upsilon}_f^{-3} >_{Av^{-1}}$ are the refractive index and integral.

$\int \varepsilon d \ln \bar{\upsilon}$ was determined from the plot of the absorptivity against the logarithm of emitted energy. Quantum yield Φ bears the following relation with radiative and non-radiative rate constants,

$$\Phi = \frac{K_r}{(K_{nr} + K_r)} \tag{2}$$

The non-radiative rate constant is given by Eq. (3),

$$K_{nr} = \frac{(1-\Phi)}{\tau} \tag{3}$$

The following equation is used to get oscillator strength f,

$$f = \frac{4.32 \times 10^{-9}}{n} \int \varepsilon(\vartheta) dv \tag{4}$$

where n refractive index and $\int \varepsilon(\vartheta) dv$ area of the absorption coefficient.

Fig. S1 and Table S1 shows nonradiative decay found increases from nonpolar to polar solvents. Radiative decay trend was random with solvent polarity. Fluorescence lifetime shows decreases in a polar solvent.

Solvent Polarity Parameter

The Stoke shift and emission correlation of 6a, 6b and 6c were studied using Lippert Mataga, and Weller's polarity plots [12, 24]. Lippert Mataga plot gives the relation between Stokes shift and orientation polarizability, Eq. (5),

$$\Delta\vartheta = \frac{2\left(\mu_e - \mu_g\right)^2}{hca_0^3} f1 + constant \tag{5}$$

where $\Delta\vartheta$, μ_g, μ_e, h, c and a_0 are Stokes shift in cm^{-1}, dipole moment at the ground state, dipole moment at the excited state, Planck constant, speed of light and the d Onsagar radii, $f1$ is obtained as,

$$f1 = \frac{\epsilon - 1}{2\epsilon + 1} - \frac{n^2 - 1}{2n^2 + 1} \tag{6}$$

Mac Rae model [25] is the slightly improvised version of the Lippert Mataga model which considers solute polarizability along with the solvent polarizability.

$$\Delta\vartheta = \frac{2\left(\mu_e - \mu_g\right)^2}{hca_0^3} f2 + constant \tag{7}$$

where $f2$,

$$f2 = \frac{\epsilon - 1}{\epsilon + 2} - \frac{n^2 - 1}{n^2 + 1} \tag{8}$$

Weller equation account frequency of emission.

$$\vartheta_f = \frac{2\mu_e^2}{hca_0^3} f3 + constant \tag{9}$$

where $f3$,

$$f3 = \frac{\epsilon - 1}{2\epsilon + 1} - \frac{n^2 - 1}{4n^2 + 2} \tag{10}$$

Lippert-Mataga equation shows poor linear fit for 6a with regression 0.18. Compound 6b and 6c show regression 0.94 and 0.90 respectively. The same trend was observed in Mc Rae plots. Regression observed 0.19, 0.96 and 0.87 for 6a, 6b and 6c. Good regression coefficient observed for Weller plots are 0.75, 0.97 and 0.88 for 6a, 6b and 6c respectively. It suggests good charge transfer occur from donor to acceptor in all compounds (Fig. 3).

Estimation of the Dipole Moment

The solvatochromic behavior of the compounds can be associated with large changes in dipole moment during transitions between two electronic states S_0 and S_1. The Stoke shift is

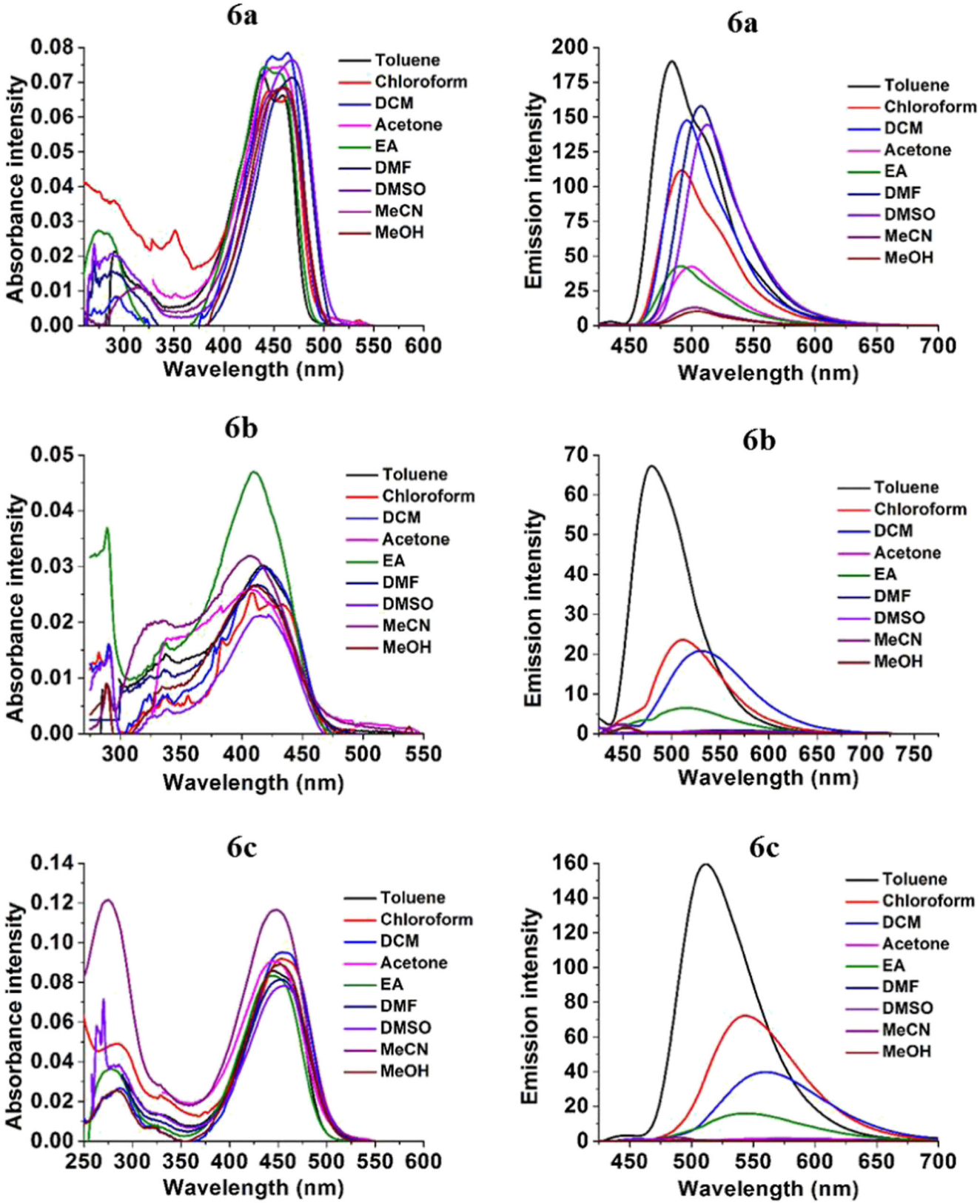

Fig. 2 Absorption and emission graphs of 6a, 6b and 6c

Table 1 Optical properties of 6a, 6b and 6c

	λ_{abs} (nm)	λ_{abs} (cm^{-1})	FWHM (nm)	FWHM (cm^{-1})	λ_{ems} (nm)	λ_{ems} (cm^{-1})	Stokes shift (nm)	Stokes shift (cm^{-1})	ε^{max}	ϕ
6a										
Toluene	438	22,831	62	3218	484	20,661	46	2170	72,180	0.32
Chloroform	444	22,523	68	3469	492	20,325	48	2197	67,430	0.24
DCM	464	21,552	61	3033	496	20,161	32	1390	78,490	0.28
Acetone	456	21,930	65	3277	500	20,000	44	1930	74,480	0.11
EA	442	22,624	62	3189	491	20,367	49	2258	74,450	0.09
DMF	467	21,413	60	2860	508	19,685	41	1728	71,370	0.27
DMSO	467	21,413	63	3011	513	19,493	46	1920	76,370	0.29
MeCN	457	21,882	63	3147	502	19,920	45	1962	68,380	0.05
MeOH	460	21,739	59	2906	504	19,841	44	1898	68,590	0.04
6b										
Toluene	418	23,923	77	4610	480	20,833	62	3090	7550	0.21
Chloroform	408	24,510	70	4073	511	19,569	103	4940	6327	0.11
DCM	417	23,981	72	4232	531	18,832	114	5148	7445	0.09
Acetone	406	24,631	111	7507	551	18,149	145	6482	6525	0.07
EA	410	24,390	69	4205	515	19,417	105	4973	11,745	0.02
DMF	413	24,213	77	4678	559	17,889	146	6324	6680	0.01
DMSO	408	24,510	64	3756	558	17,921	150	6589	5357	0.02
MeCN	408	24,510	129	9324	561	17,825	153	6684	7985	0.01
MeOH	409	24,450	76	4628	558	17,921	149	6529	6640	0.01
6c										
Toluene	445	22,472	68	3454	511	19,569	66	2902	85,860	0.27
Chloroform	453	22,075	72	3563	544	18,382	91	3693	91,950	0.19
DCM	454	22,026	69	3405	561	17,825	107	4201	95,190	0.16
Acetone	445	22,472	74	3832	572	17,483	127	4989	90,690	0.11
EA	445	22,472	68	3501	544	18,382	99	4090	83,340	0.02
DMF	451	22,173	71	3568	586	17,065	135	5108	81,390	0.04
DMSO	457	21,882	72	3578	573	17,452	116	4430	78,280	0.01
MeCN	447	22,371	73	3754	593	16,863	146	5508	116,580	0.03
MeOH	452	22,124	69	3466	598	16,722	146	5401	89,230	0.02

λ_{abs}, Absorption wavelength

λ_{ems}, Emission wavelength

FWHM, Full Width Half Maxima

ε, Molar absorptivity (M^{-1} cm^{-1})

ϕ, Quantum Yield

indicative of a change in dipole moment in the excited state. In solvatochromic method absorption and emission maxima are used to estimate the excited state dipole moments. By using the relations below, a change in dipole moment was obtained [26, 27].

$$\Delta\vartheta = m_1 f4(\epsilon, n) + const \tag{11}$$

$$\frac{\vartheta_a + \vartheta_f}{2} = m_2 f5(\epsilon, n) + const \tag{12}$$

where m_1, m_2 are slopes obtained by plot of Sthe tokes shift $\Delta\vartheta$ and $\vartheta_a + \vartheta_f/2$ versus f_4 and f_5 respectively.

$$m_1 = \frac{2\left(\mu_e - \mu_g\right)^2}{hca_0^3} \tag{13}$$

$$m_2 = \frac{2\left(\mu_e^2 - \mu_g^2\right)}{hca_0^3} \tag{14}$$

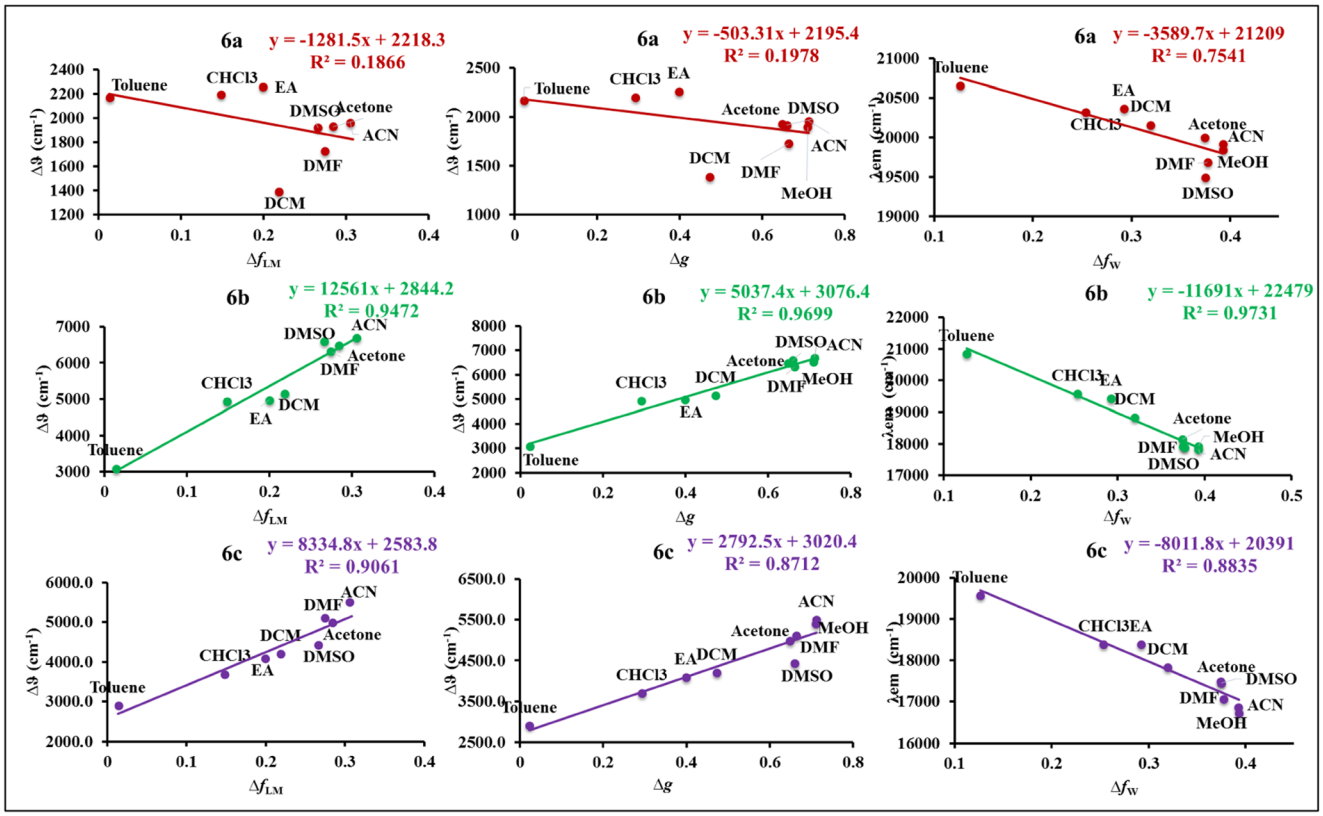

Fig. 3 Lippert-mataga (left), Mc Rae (middle) and Weller (right) Plots for 6a, 6b and 6c

ϑ_a and ϑ_f are absorption and emission frequency in cm^{-1} respectively. f_4 and f_5 Bakshiev [28] and Kawski [29] polarity functions which given as follows,

$$f4(\epsilon,n) = \frac{2n^2+1}{n^2+2}\left[\frac{\epsilon-1}{\epsilon-2} - \frac{n^2-1}{n^2+2}\right] \quad (15)$$

$$f5(\epsilon,n) = \left[\frac{2n^2+1}{2(n^2+2)}\left[\frac{\epsilon-1}{\epsilon-2} - \frac{n^2-1}{n^2+2}\right] + \frac{3(n^4-1)}{2(n^2+2)^2}\right] \quad (16)$$

Ground state dipole moment obtained by the following Eq.

$$\mu_g = \frac{m_2-m_1}{2}\left(\frac{hca_0^3}{2m_1}\right)^{\frac{1}{2}} \quad (17)$$

$$\mu_e = \frac{m_2+m_1}{2}\left(\frac{hca_0^3}{2m_1}\right)^{\frac{1}{2}} \quad (18)$$

The ratio of dipole moments obtained by the following Eq.

$$\frac{\mu_e}{\mu_e} = \frac{m_2+m_1}{m_2-m_1} \quad (19)$$

Reichardt polarity scale $\left(E_T^N\right)$

The excited state dipole moment can be obtained by solvatochromic Stoke shift and E_T^N parameter correlation [30]

Reichardt proposed E_T^N parameter by following Eq.,

$$E_T^N = \frac{E_T(Solvent)-E_T(TMS)}{E_T(Water)-E_T(TMS)} = \frac{E_{solvent}-30.7}{32.4} \quad (20)$$

Stokes shift variation with E_N^T is expressed as [31],

$$\Delta\vartheta = 11307.6\left[\left(\frac{\Delta\mu}{\Delta\mu_B}\right)^2\left(\frac{a_B}{a_0}\right)^3\right]E_T^N + constant \quad (21)$$

where $\Delta\mu_B$ and a_0 are 9D and 6.2 Å respectively for betaine dye.

From the above equation change in dipole moment, $\Delta\mu$ obtained as follow,

$$\Delta\mu = \mu_e - \mu_g = \sqrt{\frac{m_3\ X\ 81}{\left({}^{6.2}/_{a_0}\right)^3 X\ 11307.6}} \quad (22)$$

where m_3 is the slope obtained from the linear plot of Stokes shift ($\Delta\vartheta$) versus E_T^N function.

Ground state and excited state dipole moment, the ratio (μ_e/μ_g) and excess ($\Delta\mu$) obtained by the above methods and by

Lippert Mataga, Mc Rae are summarized in same Table 2. The dipole moment difference and ratio are found positive in all models indicating that dipole moment increases in the excited state. Dipole moment difference found large by Lippert Mataga model because this method does not account polarizability of the solute. Compound 6a shows small dipole moment difference than 6b and 6c, which may be due to the small effect of 7 substituted substituent on energy levels of molecules. The greater dipole moment in the excited state than ground state supports the intramolecular charge transfer in molecules.

Linear Solvation Energy Relationships and Solvatochromism

As compounds are shown emission solvatochromism, linear solvation energy relationships (LSERs) are to describe solute-solvent interactions by using Kamlet-Taft and Catalan which involve the dipolarity/polarizability and acidity and basicity parameters of the solvent [14, 15]. Effect of solvent on ϑ_{abs}, ϑ_{emm} and Stokes shift $\Delta\vartheta$ is given as,

$$y = y_0 + a\mathrm{A} + b\mathrm{B} + c\mathrm{C} + d\mathrm{D} \tag{23}$$

where y_0 is property in the gas phase, a, b and c are the adjustable regression coefficients which indicate the dependency of y to the various solvent parameters (A, B, C, and D)

The polarity/polarizability (π^*), acidity (α) and basicity (β) parameters of the solvent proposed by Kamlet and Taft in form of Eq. (24)

$$y = y_0 + a_\alpha \alpha + b_\beta \beta + c_{\pi^*}\pi^* \tag{24}$$

Table 2 Dipole moment difference and ratio of 6a, 6b and 6c

	Bilot Kawski		Transition Dipole Moment	Dipole moment difference (Δμ)					μ_e/μ_g	
	GS	ES		Bakshiev	Lippert Mataga	Mc Rae	Bilot Kawski	E_T^N	Bakshiev	Bilot Kawski
6a										
Toluene	1.04E-17	1.3E-17	10.260	2.799	4.870	3.052	2.617	1.30	1.29	1.25
$CHCl_3$	1.02E-17	1.28E-17	11.157	2.747	4.781	2.996	2.569	1.25		
CH_3CN	9.71E-18	1.22E-17	10.257	2.610	4.541	2.846	2.441	1.13		
Acetone	1.05E-17	1.31E-17	11.091	2.821	4.908	3.076	2.638	1.32		
EA	1.01E-17	1.27E-17	10.160	2.725	4.743	2.972	2.549	1.23		
DMF	9.84E-18	1.23E-17	9.539	2.646	4.604	2.885	2.474	1.16		
DMSO	1.02E-17	1.28E-17	10.660	2.747	4.781	2.996	2.569	1.25		
6b										
Toluene	7.29E-19	9.06E-18	4.340	8.300	15.774	9.989	8.334	6.18	11.85	12.43
$CHCl_3$	7.36E-19	9.16E-18	3.311	8.386	15.936	10.091	8.419	6.31		
CH_3CN	7.83E-19	9.75E-18	4.846	8.926	16.963	10.742	8.962	7.15		
Acetone	7.42E-19	9.23E-18	4.059	8.450	16.058	10.169	8.484	6.41		
EA	7.47E-19	9.3E-18	4.992	8.514	16.181	10.246	8.548	6.51		
DMF	7.47E-19	9.3E-18	4.050	8.514	16.181	10.246	8.548	6.51		
DMSO	7.38E-19	9.18E-18	2.912	8.407	15.977	10.117	8.441	6.34		
6c										
Toluene	2.12E-18	9.11E-18	13.391	6.992	11.929	7.744	6.992	12.19	5.61	4.29
$CHCl_3$	2.14E-18	9.2E-18	17.666	7.062	12.049	7.822	7.062	12.43		
CH_3CN	2.08E-18	8.95E-18	22.576	6.870	11.721	7.609	6.870	11.77		
Acetone	2.1E-18	9.02E-18	13.719	6.922	11.810	7.667	6.922	11.95		
EA	2.05E-18	8.8E-18	14.688	6.749	11.514	7.475	6.749	11.36		
DMF	2.12E-18	9.11E-18	13.222	6.992	11.929	7.744	6.992	12.19		
DMSO	2.08E-18	8.93E-18	16.008	6.853	11.692	7.590	6.853	11.71		

where α, β and π^* are respectively solvent acidity, solvent basicity and solvent polarity/polarizability.

Further Catalan used four empirical solvent scales and is expressed in form of Eq. (13),

$$y = y_0 + a_{SA}SA + b_{SB}SB + c_{SP}SP + d_{SdP}SdP \quad (25)$$

where, SA, SB, SP, and SdP are respectively solvent acidity, solvent basicity, solvent polarizability and solvent dipolarizability.

Multilinear regression analysis was done with nine solvents. From results (Table S2-S7), it is seen that in emission correlation, the regression coefficient is larger in the case of Catalan parameter than Kamlet-Taft parameter. For absorption, emission, and Stokes shift correlation high standard errors were observed. Compound 6a exhibits better regression coefficient for absorption, emission and Stokes shift ($r = 0.94$, 0.94, 0.74 respectively for Kamlet Taft parameter). The negative sign of coefficient c and $d$explains that solvent polarizability and dipolarity are the key factors for the observed solvatochromic shift. The plot of experimental and predicted emission values (Fig. 4 and S2) shows good correlation with regression coefficient $r = 0.94$, 0.95 for 6a, 0.76, 0.88 for 6b and 0.73 and 0.82 for 6c respectively in Kamlet-Taft and Catalan parameter.

General Mulliken Hush Analysis (GMH)

Donor to acceptor charge transfer characteristics is evaluated by General Mulliken Hush (GMH) analysis given by Coe et al. [32]. GMH analysis in its two-state analysis of ICT states,

$$\Delta\mu_{ab}^2 = \Delta\mu_{ge}^2 + 4\mu_{ge}^2 \quad (26)$$

where μ_{ge} is the transition dipole moment, expressed as,

$$\mu_{ge}^2 = \frac{3e^2h}{8\pi^2mc} \times \frac{f}{\vartheta_{eg}} \quad (27)$$

where, e, h, m, c, f, and ϑ are ca harge on the electron, Planks constant, the mass of the electron, speed of light, oscillator strength, and frequency of the absorption.

The degree of delocalization (Cb^2) and electronic coupling matrix (H_{DA}) between charge transfer excited states are important expressed as,

$$C_b^2 = \frac{1}{2}\left(1 - \sqrt{\frac{\Delta\mu_{ge}^2}{\Delta\mu_{ge}^2 + 4\mu_{ge}^2}}\right) \quad (28)$$

$$H_{DA} = \frac{\Delta E_{ge}\mu_{ge}}{\Delta\mu_{ab}} = \frac{\Delta E_{ge}\mu_{ge}}{\sqrt{\Delta\mu_{ge}^2 + 4\mu_{ge}^2}} \quad (29)$$

where, ΔE_{ge} vertical excitation energy, $\Delta\mu_{ge}$ the excess dipole moments, $\Delta\mu_{ab}$ depends on the difference in adiabatic state dipole moment and the transition dipole moment.

The assumption here is that the adiabatic states contain three diabatic states viz, ground (S_0), local excited (LE), and charge transfer (CT) state with the transfer of localized electron. Thus, the extent of charge separation generated because of the interactions through π-bridge is expressed as,

$$R_{DA} = 2.06 \times 10^{-2}\frac{\sqrt{\Delta E_{ge}\varepsilon_{max}\Delta\nu_{1/2}}}{H_{DA}} \quad (30)$$

where, R_{DA}, ε_{max}, $\Delta\nu_{1/2}$, H_{DA} are distance between the centroids of the donor-acceptor orbitals (Å), absorptivity (M^{-1} cm^{-1}), bandwidth (cm^{-1}), electronic coupling matrix $(cm)^{-1}$, and ΔE_{ge} same as above.

The transition dipole moment ($\Delta\mu_{eg}$), the degree of delocalization (Cb^2), electron coupling matrix (H_{DA}) and donor-acceptor separation (R_{DA}) are summarized in Table 3. It reveals that the values of the degree of delocalization ($C^2{}_b$) tend towards zero suggested their significant charge transfer occurred. The electron

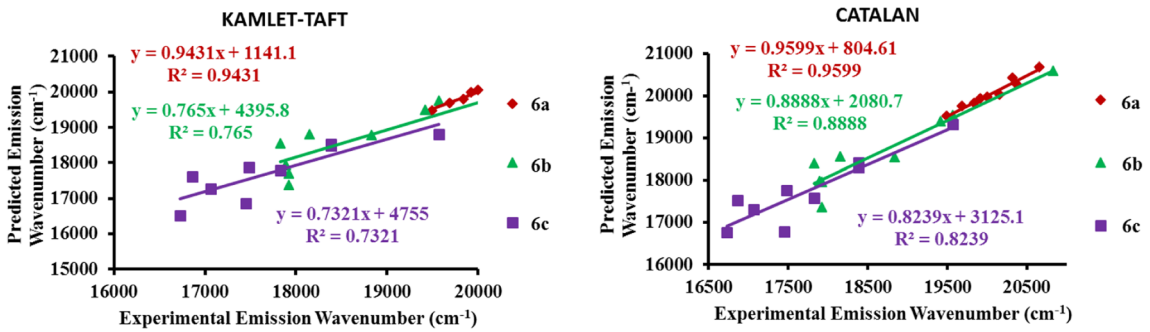

Fig. 4 Plot of experimental and predicted emission wavenumber

Table 3 Linear optical and charge transfer characteristics of 6a, 6b and 6c

	a_0 [a] (Å)	IAC[b] (M^{-1} cm^{-1})	f[c]	$\Delta\mu_{CT}$ [d] Debye	$\Delta\mu_{ge}$ [e] Debye	$\Delta\mu_{ab}$ [f] Debye	Cb^2 [g]	H_{DA} [h]	R_{DA} [i]
6a									
Toluene	5.71	257,195,054	1.129	4.870	10.260	21.090	0.385	11,107.014	4.271
$CHCl_3$	5.64	299,999,276	1.317	4.781	11.157	22.820	0.395	11,011.361	4.294
CH_3CN	5.45	246,348,951	1.081	4.541	10.257	21.011	0.392	10,682.304	4.185
Acetone	5.74	288,660,039	1.267	4.908	11.091	22.718	0.392	10,705.925	4.452
EA	5.61	249,930,412	1.097	4.743	10.160	20.867	0.386	11,016.162	4.334
DMF	5.5	208,508,252	0.915	4.604	9.539	19.626	0.383	10,407.885	4.138
DMSO	5.64	260,373,896	1.143	4.781	10.660	21.849	0.391	10,447.188	4.375
6b									
Toluene	5.84	48,213,798	0.212	15.774	4.340	18.004	0.062	5766.552	3.260
$CHCl_3$	5.88	28,747,241	0.126	15.936	3.311	17.257	0.038	4702.106	3.482
CH_3CN	6.13	61,593,878	0.270	16.963	4.846	19.537	0.066	6079.585	4.577
Acetone	5.91	43,419,636	0.191	16.058	4.059	17.993	0.054	5555.919	4.073
EA	5.94	65,032,933	0.285	16.181	4.992	19.013	0.074	6403.540	3.531
DMF	5.94	42,508,238	0.187	16.181	4.050	18.095	0.053	5419.831	3.306
DMSO	5.89	22,247,982	0.098	15.977	2.912	17.005	0.030	4197.719	3.446
6c									
Toluene	6	431,196,840	1.893	11.929	13.391	29.318	0.297	10,263.754	5.181
$CHCl_3$	6.04	737,199,594	3.236	12.049	17.666	37.329	0.339	10,446.746	5.303
CH_3CN	5.93	1,220,151,600	5.356	11.721	22.576	46.649	0.374	10,826.816	5.953
Acetone	5.96	452,624,837	1.987	11.810	13.719	29.873	0.302	10,320.527	5.578
EA	5.86	518,781,700	2.277	11.514	14.688	31.552	0.318	10,461.036	5.043
DMF	6	414,799,279	1.821	11.929	13.222	29.010	0.294	10,105.729	5.173
DMSO	5.92	600,013,407	2.634	11.692	16.008	34.083	0.328	10,277.054	4.963

[a] Onsagar Radii

[b] Integrated Absorption Coefficient

[c] Oscillator strength

[d] Difference between ground and excited state dipole moments evaluated using Lippert-Mataga solvent polarity parameter

[e] Transition dipole moment

[f] Difference in diabatic state dipole moments and the transition dipole moment

[g] Degree of delocalization

[h] Electronic coupling matrix

[i] Donor-acceptor separation

coupling matrix (H_{DA}) has the trend as 6a > 6c > 6b. Charge separation (R_{DA}) is more in 6c as compared to 6a and in 6b. It indicates that diphenyl substituent leads to more charge separation than N,N-diethylamine and carbazole substituent.

Time Dependent Density Functional Theory (TD-DFT) Study

The geometry of the compounds are optimized at the ground and excited state with global hybrid B3LYP and basis set 6-31G(d). The bond lengths bond angles and dihedral angles are summarized in the table. From the ground state and excited state geometry, it was observed that coumarin ring and benzothiazole ring are planar, but the geometries differ. In 6a dihedral angle N, N-diethyl amine group and coumarin benzene ring change from 2.15^0 to 23.45^0. In 6b dihedral angle from 49.21 to 89.78 carbazole ring completely perpendicular to coumarin ring in an excited state. Same observation for 6c. Two phenyl rings are perpendicular to the coumarin ring (Fig. 5). Single and double bond from C_1 to C_{30} bond lengths in the ground state, decreases and increases respectively in an excited state (Table 4) shows electron delocalization.

Vertical excitation, oscillator strength, orbital contribution are listed in Table 5. Vertical excitation of the compounds is in good agreement to experimental absorption values. In all the compounds and solvents HOMO to LUMO transition takes place which corresponds to π-π* transition.

Electron density distributions of molecules are studied by frontier molecular orbital approach (FMO). Fig 6 indicates HOMO- LUMO of the compounds in chloroform at the ground state. From Fig. 6 it is observed that in 6a, electron density located all over molecule in HOMO while in LUMO electron density concentrated on coumarin ring. In 6b and 6c, electron density located

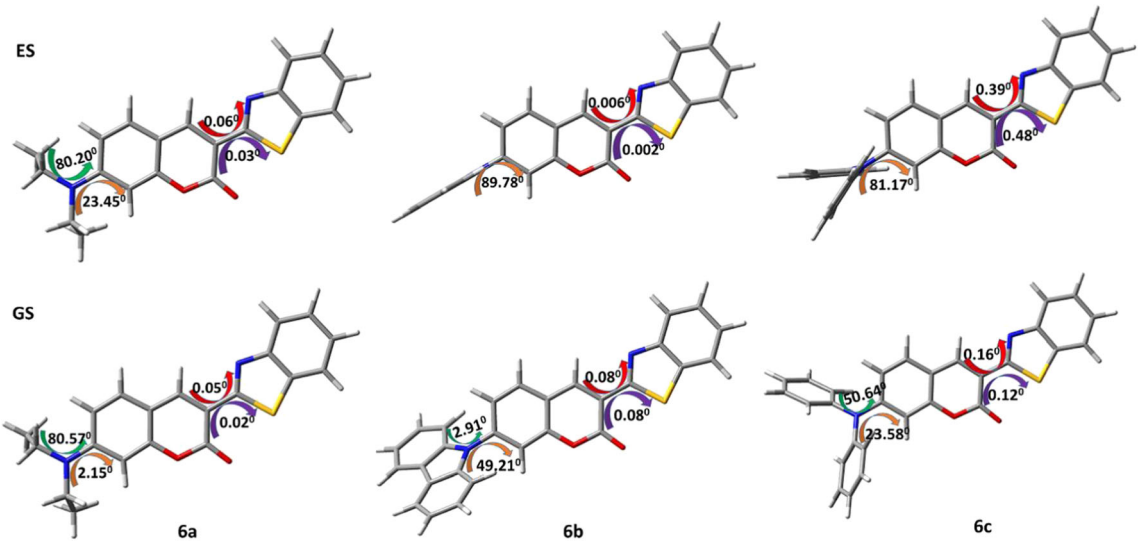

Fig. 5 optimized geometry at the ground and excited state

at benzthiazole group and in LUMO it shifted to the coumarin ring. Trend of HOMO-LUMO gap is, 6a > 6b > 6c.

Nonlinear Optical Properties (NLO)

Nonlinear optical properties of the compounds were obtained from DFT and solvatochromic methods.

Table 4 Bond length and dihedral angle obtained from the optimized geometry of 6a, 6b and 6c

	6a		6b		6c	
	GS	ES	GS	ES	GS	ES
Bond Length (Å)						
C_1-N_{14}	1.371	1.376	1.411	1.442	1.395	1.453
C_1-C_5	1.433	1.431	1.413	1.402	1.423	1.400
C_5-C_4	1.376	1.377	1.383	1.384	1.378	1.387
C_3-C_4	1.414	1.427	1.411	1.427	1.414	1.425
C_3-C_8	1.414	1.403	1.426	1.402	1.418	1.406
C_8-C_{10}	1.377	1.430	1.369	1.418	1.375	1.415
C_{10}-C_{35}	1.460	1.414	1.465	1.439	1.462	1.439
C_{35}-N_{40}	1.306	1.342	1.305	1.316	1.306	1.317
C_{40}-C_{29}	1.381	1.354	1.380	1.378	1.380	1.377
C_{29}-C_{30}	1.416	1.434	1.417	1.418	1.416	1.419
C_{35}-S_{41}	1.786	1.800	1.781	1.803	1.784	1.802
S_{41}-C_{30}	1.753	1.754	1.751	1.758	1.753	1.757
Dihedral angle (Degree)						
C_{15}-N_{14}-C_1-C_{42}	2.151	2.457	49.214	89.782	23.582	81.170
C_8-C_{10}-C_{35}-N_{40}	0.058	0.070	0.085	0.006	0.162	0.397
C_{11}-C_{10}-C_{35}-C_{41}	0.022	0.032	0.081	0.003	0.126	0.482
C_{25}-C_{22}-N_{14}-C_1	80.574	80.205	2.919	0.171	50.641	29.830

Spectroscopic Approach

The chromophores having D-A systems possess first excited state as a low lying CT state. The dominant component of the first order polarizability, α_{CT} and is therefore obtained by [33],

$$\alpha_{CT} = \alpha_{XX} = 2\,\frac{\mu_{eg}^2}{E_{eg}} = 2\,\frac{\mu_{eg}^2 \lambda_{eg}}{hc} \tag{31}$$

where X, μ_{eg}, E_{eg}, λ_{eg}, h, c are charge transfer direction, transition dipole moment, ground to excited transition state energy, the ground to excited state transition energy, Planck's constant and velocity of light in vacuum respectively.

The first order polarizability α_{CT} found 46.36×10^{-24} e.s.u, 7.52×10^{-24} e.s.u and 80.23×10^{-24} e.s.u for 6a, 6b and 6c respectively in toluene.

Two level model based on Oudar equation was used to calculate first order hyperpolarizability [34, 35]. β_{CT} expressed as Eq. (32)

$$\beta_{CT} = \beta_{xxx} = \frac{3}{2h^2c^2} \times \frac{\vartheta_{eg}^2 \mu_{eg}^2 \Delta\mu_{CT}}{\left(\vartheta_{eg}^2 - \vartheta_L^2\right)\left(\vartheta_{eg}^2 - 4\vartheta_L^2\right)} \tag{32}$$

where ϑ_{eg}, $\Delta\mu_{CT}$, ϑ_L, are the frequency, excess dipole moment and frequency of the incident radiation to which β_{CT} value would be referred to.

If $\vartheta_{L=0}$ under static conditions, the Eq. (20) will be,

$$\beta_{CT} = \beta_{xxx} = \frac{3\mu_{eg}^2 \Delta\mu_{CT}}{2(E_{max})^2} \tag{33}$$

In toluene the first order hyperpolarizability β_{CT} observed 37.29×10^{-30} e.s.u, 16.68×10^{-30} e.s.u and 160.61×10^{-30} e.s.u for 6a, 6b and 6c respectively.

Table 5 Vertical excitation, oscillator strength, orbital contribution and HOMO-LUMO for 6a, 6b and 6c

	λabs[a]	λabs[b]	*f*[f]	Orbital contribution	H-L
6a					
Toluene	438	421	1.278	0.70446	92 - > 93
$CHCl_3$	444	423	1.275	0.70426	92 - > 93
MeCN	457	424	1.256	0.70400	92 - > 93
	456	424	1.260	0.70403	92 - > 93
Acetone					
EA	442	422	1.257	0.70417	92 - > 93
MeOH	460	423	1.251	0.70399	92 - > 93
DMF	467	426	1.281	0.70404	92 - > 93
DMSO	467	426	1.278	0.70403	92 - > 93
6b					
Toluene	418	473	0.710	0.70439	115 - > 116
$CHCl_3$	408	473	0.689	0.70442	115 - > 116
MeCN	408	472	0.654	0.70438	115 - > 116
	406	472	0.657	0.70439	115 - > 116
Acetone					
EA	410	472	0.670	0.70438	115 - > 116
MeOH	409	472	0.651	0.70437	115 - > 116
DMF	413	472	0.674	0.70444	115 - > 116
DMSO	408	473	0.671	0.70443	115 - > 116
6c					
Toluene	445	457	1.287	0.70394	116 - > 117
$CHCl_3$	453	459	1.274	0.70397	116 - > 117
MeCN	447	459	1.249	0.70399	116 - > 117
	445	460	1.253	0.70399	116 - > 117
Acetone					
EA	445	458	1.255	0.70398	116 - > 117
MeOH	452	459	1.245	0.70399	116 - > 117
DMF	451	462	1.273	0.70398	116 - > 117
DMSO	457	462	1.269	0.70398	116 - > 117

[a] Experimental absorption

[b] Vertical excitation

[f] Oscillator strength

Determination of second-order hyperpolarizability γ

γ, second order hyperpolarizability is given as [36],

$$\gamma_{SD} = 24\left[\frac{\Delta\mu^2\mu_{eg}^2}{E_{eg}^3} - \frac{\mu_{eg}^4}{E_{eg}^3} + \sum\frac{\mu_{eg}^2\mu_{e\acute{e}}^2}{E_{eg}^2E_{\acute{e}}}\right] \quad (34)$$

where $\Delta\mu$, μ_{eg}, E_{eg} are the excess dipole moment, transition dipole moment, and excitation energy,

$$E = \frac{hc}{\lambda} = hc\vartheta \quad (35)$$

g, *e* and *é* represent ground, first excited and second excited states respectively.

Here we consider the only two-state model, therefore, Eq. (34) is simplified as below.

$$\gamma_{SD} = 24\left[\frac{\Delta\mu^2\mu_{eg}^2}{E_{eg}^3} - \frac{\mu_{eg}^4}{E_{eg}^3}\right] \quad (36)$$

The second order hyperpolarizabilities γ_{SD} were found to be -91.68×10^{-36} e.s.u, -40.20×10^{-36} e.s.u and -74.30×10^{-36} e.s.u for 6a-6c in toluene.

Computational Approach

Static dipole moment μ, linear average polarizability α_0, the anisotropy of polarizability $\Delta\alpha$ and first and second hyperpolarizability β_0 and γ were calculated by a computational approach.

μ, α_0, $\Delta\alpha$, β_0, γ expressed as following Eqs. (37–42) [37–39],

Static dipole moment (μ)

$$\mu = \left(\mu_x^2 + \mu_y^2 + \mu_z^2\right)^{\frac{1}{2}} \tag{37}$$

Mean polarizability α_0,

$$\alpha_0 = \frac{1}{3}\left(\alpha_{xx} + \alpha_{yy} + \alpha_{zz}\right) \tag{38}$$

Anisotropy of polarizability $\Delta\alpha$,

$$\Delta\alpha = 2^{\frac{-1}{2}}\left[\left(\alpha_{xx}-\alpha_{yy}\right)^2 + \left(\alpha_{yy}-\alpha_{zz}\right)^2 + \left(\alpha_{zz}-\alpha_{xx}\right)^2 + 6\alpha_{xx}^2\right]^{\frac{1}{2}} \tag{39}$$

The total first hyperpolarizability β_0,

$$\beta_0 = \sqrt{\beta_x^2 + \beta_y^2 + \beta_z^2} \tag{40}$$

$$\beta_0 = \left[\left(\beta_{xxx} + \beta_{xyy} + \beta_{xzz}\right)^2 + \left(\beta_{yyy} + \beta_{yxx} + \beta_{yzz}\right)^2 + \left(\beta_{zxx} + \beta_{zyy} + \beta_{zzz}\right)^2\right]^{\frac{1}{2}} \tag{41}$$

$$\gamma = \frac{1}{5}\left[\gamma_{xxx} + \gamma_{yyyy} + \gamma_{zzzz} + 2\left(\gamma_{xxyy} + \gamma_{xxzz} + \gamma_{yyzz}\right)\right] \tag{42}$$

By using computational approach values obtained from μ, α_0, β_0, γ in various solvents are summarized in Table 6**.** The static dipole moment and first hyperpolarizability increase from non-polar to the polar solvent for all compounds. Polarizability and second hyperpolarizability decreases for 6a and increases for 6b and 6c from nonpolar to polar solvent. Highest static dipole moment observed is 11.42 D for 6a in DMSO. 6c shows highest α_0, β_0 and γ are 88.89 X 10^{-24}, 207.35 X 10^{-30} and 1043 X 10^{-36} e.s.u respectively in DMSO.

Conclusion

We have examined the effect of different substituents on linear and nonlinear optical properties. By using solvatochromic models charge transfer characteristics were evaluated. Ground and excited state geometry of the compounds were optimized by B3LYP-6/31G(d). Spectroscopic properties supported by DFT study. Effect of the substituent on ground and excited state dipole moment was evaluated. Dipole moment difference and ratio were calculated using different models to support charge transfer characteristics. Compound with diphenylamine substituent at 7 position shows red shifted absorption, emission, high donor-acceptor charge separation, low HOMO-LUMO band gap and large hyperpolarizability compared to other compounds with N,N-diethylamine and carbazole substituent. In conclusion compound, 6c is a better candidate as a linear and nonlinear chromophore.

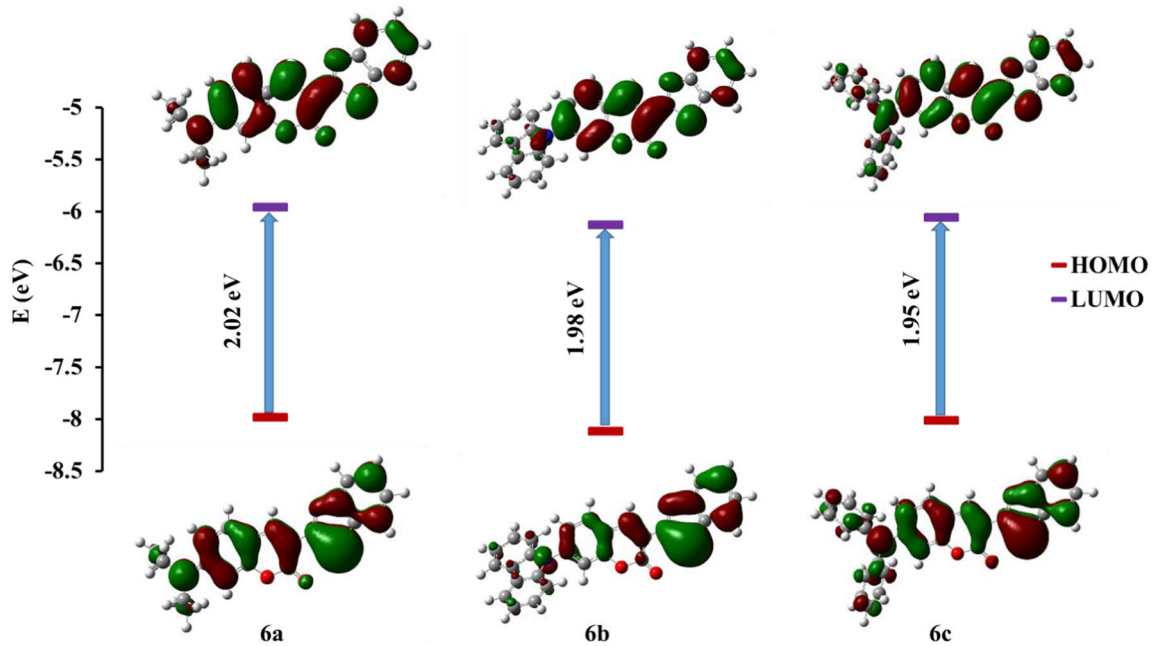

Fig. 6 FMO diagram of 6a, 6b and 6c

Table 6 Measured and calculated spectroscopic and theoretical (CAM-B3LYP/6–311 + G(d,p)) linear and non-linear optical properties of 6a, 6b and 6c

	μ^a	$\alpha_{CT}{}^b$	$\alpha_0{}^c$	$\beta_{CT}{}^d$	$\beta_0{}^e$	$\gamma_{SD}{}^f$	γ^g	$\mu\beta_{CT}{}^h$	$\mu\beta_0{}^i$
	Debye	× 10^{-24} (e.s.u)	x 10^{-24} (e.s.u)	× 10^{-30} (e.s.u)	x 10^{-30} (e.s.u)	× 10^{-36} (e.s.u)	x 10^{-36} (e.s.u)	× 10^{-48} (e.s.u)	x 10^{-48} (e.s.u)
6a									
Toluene	5.20	46.36	81.17	37.29	81.14	−91.68	742.32	193.78	421.63
$CHCl_3$	10.33	55.57	71.55	44.48	125.58	−140.70	436.40	459.64	1297.76
MeCN	11.37	48.34	68.47	37.83	168.42	−107.94	582.41	430.20	1915.16
Acetone	11.24	56.40	67.63	47.60	162.55	−146.61	561.90	534.93	1826.62
EA	10.56	45.88	63.53	36.27	134.42	−91.47	465.95	383.02	1419.66
DMF	11.38	42.73	68.52	34.64	168.76	−82.21	583.59	394.17	1920.25
DMSO	11.42	53.36	68.75	44.92	170.38	−133.50	589.27	512.76	1944.89
6b									
Toluene	4.57	7.92	72.87	19.68	62.15	40.20	557.79	89.89	283.86
$CHCl_3$	5.00	4.50	78.51	11.02	75.42	22.99	684.25	55.09	376.85
MeCN	5.52	9.63	85.64	25.14	89.58	53.57	834.92	138.82	494.58
Acetone	5.45	6.73	84.67	16.53	87.88	33.82	815.39	90.12	479.02
EA	5.11	10.27	80.01	25.70	78.71	51.70	717.21	131.30	402.19
DMF	5.53	6.81	85.69	17.17	89.67	36.04	836.02	94.85	495.45
DMSO	5.54	3.48	85.96	8.55	90.12	18.07	841.29	47.42	499.60
6c									
Toluene	7.57	80.23	74.71	160.61	123.30	−74.30	620.34	1216.41	933.86
$CHCl_3$	8.26	142.15	80.77	292.57	159.14	−615.30	795.60	2418.01	1315.28
MeCN	9.06	229.08	88.54	452.59	205.32	−2153.72	1032.22	4101.17	1860.49
Acetone	8.96	84.22	87.49	166.91	199.15	−102.73	999.59	1495.68	1784.60
EA	8.44	96.53	82.39	186.51	159.14	−200.89	844.49	1574.34	1343.32
DMF	9.07	79.28	88.60	160.84	205.62	−66.25	1033.70	1458.62	1864.79
DMSO	9.10	117.75	88.89	237.24	207.35	−371.56	1043.00	2157.69	1885.90

[a] Total static dipole moment (by DFT)

[b] Experimental first order polarizability

[c] First order polarizability (by DFT)

[d] Experimental first order hyperpolarizability

[e] First order hyperpolarizability (by DFT)

[f] Experimental second order hyperpolarizability

[g] Second order hyperpolarizability (by DFT)

[h] Quadratic hyperpolarizability by the solvatochromic method

[i] Quadratic hyperpolarizability by the computational method

Acknowledgments Author Archana A. Bhagwat is thankful to UGC for research fellowship.

References

1. Marini A, Muñoz-Losa A, Biancardi A, Mennucci B (2010) What is Solvatochromism? J Phys Chem B 114:17128–17135. https://doi.org/10.1021/jp1097487
2. Liu X, Cole JM, Sing K (2013) Low solvent effects on the UV−Vis absorption and emission of optoelectronic Coumarins: a comparison of three empirical Solvatochromic models. J Phys Chem C 117: 14731–14741. https://doi.org/10.1021/jp310397z
3. Maity B, Chatterjee A, Seth D (2014) Photophysics of a Coumarin in different solvents: use of different Solvatochromic models. Photochem Photobiol 90:734–746. https://doi.org/10.1111/php.12258
4. Abdel-Mottaleb MSA, Antonious MS, Ali MMA, Ismail LFM, El-Sayed BA, Sherief AMK (1992) Photophysics and dynamics of coumarin laser dyes and their analytical implications. Proc Indian Acad Sci (Chem Sci) 104:185–196
5. Enculescu M, Evanghelidis A, Enculescu I (2018) White-light emission of dye-doped polymer submicronic fibers produced by electrospinning. Polymers 10:737. https://doi.org/10.3390/polym10070737
6. Finke JH, Richter C, Gothsch T, Kwade A, Büttgenbach S, Müller-Goymann CC (2014) Coumarin 6 as a fluorescent model drug: how to identify properties of lipid colloidal drug delivery systems via fluorescence spectroscopy? Eur J Lipid Sci Technol 116:1234–1246. https://doi.org/10.1002/ejlt.201300413
7. Pretor S, Bartels J, Lorenz T, Dahl K, Finke JH, Peterat G, Krull R, Al-Halhouli AT, Dietzel A, Büttgenbach S, Behrends S, Reichl S, Müller-Goymann CC (2015) Cellular uptake of Coumarin-6 under microfluidic conditions into HCE-T cells from Nano scale formulations. Mol Pharm 12: 34–45. https://doi.org/10.1021/mp500401t
8. Warde U, Sekar N (2017) Benzocoumarin-Styryl hybrids: aggregation and viscosity induced emission enhancement. J Fluoresc 27: 1747–1758. https://doi.org/10.1007/s10895-017-2113-3
9. Avhad KC, Patil DS, Gawale YK, Chitrambalam S, Sreenath MC, Joe IH, Sekar N (2018) Large stokes shifted far-red to NIR emitting D-π-a Coumarins: combined synthesis, experimental, and computational investigation of spectroscopic and non-linear optical

properties. Chem Select 3:4393–4405. https://doi.org/10.1002/slct.201800063
10. Lanke SK, Sekar N (2016) AIE based Coumarin chromophore-evaluation and correlation between Solvatochromism and solvent polarity parameters. J Fluoresc 26:497–511. https://doi.org/10.1007/s10895-015-1735-6
11. Tathe AB, Sekar N (2016) Red emitting NLOphoric 3-styryl coumarins: experimental and computational studies. Opt Mater 51: 121–127. https://doi.org/10.1016/j.optmat.2015.11.031
12. Mataga N, Kaifu Y, Koizumi M (1956) Solvent effects upon fluorescence spectra and the dipole moments of excited molecules. Bull Chem Soc Jpn 29:465–470. https://doi.org/10.1246/bcsj.29.465
13. Reichardt C (1994) Solvatochromic dyes as solvent polarity indicators. Chem Rev 94: 2319–2358. 10.1009–2665/94/0794–2319
14. Kamlet MJ, Taft RW (1976) The solvatochromic comparison method. I. the β-scale of solvent hydrogen bond acceptor (HBA) basicities. J Am Chem Soc 98:377–383. https://doi.org/10.1021/ja00418a009
15. Catalàn J (2009) Toward a generalized treatment of the solvent effect based on four empirical scales: Dipolarity (SdP, a new scale), polarizability (SP), acidity (SA), and basicity (SB) of the medium. J Phys Chem B 113:5951–5960. https://doi.org/10.1021/jp8095727
16. Gieseking RL, Mukhopadhyay S, Risko C, Brédas J-L (2014) Impact of the nature of the excited-state transition dipole moments on the third-order nonlinear optical response of Polymethine dyes for all-optical switching applications. ACS Photonics 1:261–269. https://doi.org/10.1021/ph4001444
17. Liu X, Cole JM, Waddell PG, Lin T-C, Radia J, Zeidler A (2012) Molecular origins of optoelectronic properties in Coumarin dyes: toward designer solar cell and laser applications. J Phys Chem A 116:727–737. https://doi.org/10.1021/jp209925y
18. Hara K, Sato T, Katoh R, Furube A, Ohga Y, Shinpo A, Suga S, Sayama K, Sugihara H, Arakawa H (2003) Molecular Design of Coumarin Dyes for efficient dye-sensitized solar cells. J Phys Chem B 107:597–606. https://doi.org/10.1021/jp026963x
19. Padalkar VS, Patil VS, Gupta VD, Phatangare KR, Umape PG, Sekar N (2011) Synthesis, characterization, thermal properties, and antimicrobial activities of 5-(Diethylamino)-2-(5-nitro-1H-benzimidazol-2-yl)phenol and its transition metal complexes. ISRN Org Chem 2011:738361. https://doi.org/10.5402/2011/738361
20. Yu T, Zhao M, Li A, Zhao Y, Zhang H, Fan D (2013) Synthesis and photoluminescent properties of 7-N,N-diphenylamino-3-benzoheterocyclic coumarin derivatives. Res Chem Intermed 39: 2259–2266. https://doi.org/10.1007/s11164-012-0755-y
21. Yin H, Zhang B, Yu H, Zhu L, Feng Y, Zhu M, Guo Q, Meng X (2015) Two-photon fluorescent probes for biological Mg2+ detection based on 7-substituted Coumarin. J Org Chem 80:4306–4312. https://doi.org/10.1021/jo502775t
22. Raju BB, Costa SMB (1999) Photophysical properties of 7-diethylaminocoumarin dyes in dioxane-water mixtures: hydrogen bonding, dielectric enrichment and polarity effects. Phys Chem Chem Phys 1:3539–3547
23. Satpati AK, Kumbhakar M, Nath S, Pal H (2009) Photophysical properties of Coumarin-7 dye: role of twisted intramolecular charge transfer state in high polarity Protic solvents. Photochem Photobiol 85:119–129. https://doi.org/10.1111/j.1751-1097.2008.00405.x
24. Beens H, Knibbe H, Weller A (1967) Dipolar nature of molecular complexes formed in the excited state. J Chem Phys 47:1183–1184. https://doi.org/10.1063/1.1712006
25. Mc Rae EG (1957) Theory of solvent effects on molecular electronic spectra. Frequency shifts. J Phys Chem 61:562–572. https://doi.org/10.1021/j150551a012
26. Evale BG, Hanagodimath SM, Khan IA, Kulkarni MV (2009) Estimation of dipole moments of some biologically active coumarins by solvatochromic shift method based on solvent polarity parameter. EN Spectrochim Acta Part A 73:694–700. https://doi.org/10.1016/j.saa.2009.03.016
27. Husaina MM, Sindhua R, Tandon HC (2012) Photophysical properties and estimation of ground and excited state dipole moments of 7-diethylamino and 7-diethylamino-4-methyl coumarin dyes from absorption and emission spectra. Eur J Chem 3:87–93. https://doi.org/10.5155/eurjchem.3.1.87-93.519
28. Bakshiev NG (1964) Universal intermolecular interactions and their effect of the position of the electronic spectra of molecules in 2-component solutions.7. Theory (general case of isotopic solution). Opt. I Spektrosk 16:821–832
29. Kawski A (2002) On the estimation of excited-state dipole moments from solvatochromic shifts of absorption and fluorescence spectra. Z Naturforsch 57a:255–262
30. Reichardt C (2003) Solvent effects on the absorption spectra of organic compounds in solvents and solvent effects in organic chemistry, third edn. Wiley-VCH, Weinheim
31. Ravi M, Soujanya T, Samanta A, Radhakrishnan TP, Excited-state dipole moments of some Coumarin dyes from a solvatochromic method using the solvent polarity parameter, E^{N}_{T}. J. Chem Soc Faraday Trans 91:2739. https://doi.org/10.1039/FT9959102739, 1995
32. Coe BJ, Clays K, Foerier S, Verbiest T, Asselberghs I (2008) Redox-switching of nonlinear optical behavior in Langmuir - Blodgett thin films containing a ruthenium (II) ammine complex. J Am Chem Soc 130:3286–3287. https://doi.org/10.1021/ja711170q
33. Abbotto A, Beverina L, Bradamante S, Facchetti A, Klein C, Pagani GA, Redi-abshiro M (2003) A distinctive example of the cooperative interplay of structure and environment in tuning of intramolecular charge transfer in second-order nonlinear optical chromophores. Chem Eur J 9:1991–2007. https://doi.org/10.1002/chem.200204356
34. Oudar JL (1977) Optical nonlinearities of conjugated molecules. Stilbene derivatives and highly polar aromatic compounds. J Chem Phys 67:446–457. https://doi.org/10.1063/1.434888
35. Carlotti B, Flamini R, Kikaš I, Mazzucato U, Spalletti A (2012) Intramolecular charge transfer, solvatochromism and hyperpolarizability of compounds bearing ethenylene or ethynylene bridges. Chem Phys 407:9–19. https://doi.org/10.1016/j.chemphys.2012.08.006
36. Calaminici P, Jug K, Köster AM (1998) Density functional calculations of molecular polarizabilities and hyperpolarizabilities and hyperpolarizabilities. J Chem Phys 109:7756–7763. https://doi.org/10.1063/1.477421
37. Meyers F, Marder SR, Pierce BM, Brédas JL (1994) Electric field modulated nonlinear optical properties of donor-acceptor polyenes: sum-over-states investigation of the relationship between molecular polarizabilities (alpha, beta, and gamma) and bond length alternation. J Am Chem Soc 116:10703–10714. https://doi.org/10.1021/ja00102a040
38. Kothavale S, Jadhav AG, Sekar N (2017) Deep red emitting triphenylamine based coumarin-rhodamine hybrids with large stokes shift and viscosity sensing: synthesis, photophysical properties and DFT studies of their spirocyclic and open forms. Dyes Pigments 137:329–341. https://doi.org/10.1016/j.dyepig.2016.11.010
39. Strickler SJ, Berg RA (1962) Relationship between absorption intensity and fluorescence lifetime of molecules. J Chem Phys 37: 814–822. https://doi.org/10.1063/1.1733166